Vision Research 186 (2021) 34–40

Contents lists available at ScienceDirect

Vision Research

journal homepage: www.elsevier.com/locate/visres

The interaction of global motion and global form processing on the perception of implied motion: An equivalent noise approach

Mahesh R. Joshi [a,*], Anita J. Simmers [b], Seong T. Jeon [b]

[a] Eye and Vision Research Group, School of Health Professions, University of Plymouth, Plymouth, United Kingdom
[b] Vision Sciences, Department of Life Sciences, Glasgow Caledonian University, Glasgow, United Kingdom

ARTICLE INFO

Keywords:
Global motion
Global form
Implied motion
Noise
Equivalent noise paradigm

ABSTRACT

Global motion and global form are proposed to be processed through functionally differentiated independent channels along dorsal (motion) and ventral (form) pathways. However, more recent studies show significant interactions between these pathways by inducing the perception of motion (implied motion) from presenting the independent frames of static Glass patterns. The mechanisms behind such interaction are not adequately understood with studies showing a larger contribution of either a motion or form processing mechanism. In the current study, we adapted the equivalent noise paradigm to disentangle the effect of internal noise (local processing) and sampling efficiency (global processing) on global motion, global form, and the interaction of both on the perception of implied motion using physically equivalent stimuli. Six visually normal observers discriminated the direction or orientation of random dot kinematograms (RDK), static Glass patterns (Glass), and dynamic Glass patterns (*d*Glass) whose directions/orientations were determined by the means of normal distributions with a range of direction/orientation variances that served as external noise. Thresholds (τ) showed a consistent pattern across observers and external noise levels, where $\tau_{Glass} > \tau_{dGlass} > \tau_{RDK}$. Nested model comparisons where the thresholds were related to the external noise, internal noise, and the sampling efficiency revealed that the difference in performance between the tasks was best described by the change in sampling efficiency with invariable internal noise. Our results showed that the higher thresholds for implied motion compared to real motion could be due to inefficient pooling of local dipole orientation cues at global processing stages involving motion mechanisms.

1. Introduction

Global motion and global form are proposed to be predominantly processed along independent channels of dorsal and ventral streams (Braddick, Atkinson & Wattam-Bell, 2003, Braddick, et al., 2001, Braddick, et al., 2002, Livingstone & Hubel, 1987, Milner & Goodale, 2008). Random dot kinematograms (RDK) and Glass patterns (Glass, 1969) are commonly used stimuli to evaluate global motion and form processing. Glass patterns are formed when an identical set of random dot pattern is superimposed upon another, whereby one pattern is generated following a linear or nonlinear transformation of the other pattern. (Glass, 1969) A variety of different spatial patterns can be generated based on the angle of displacement by aligning the correlated pairs of dots (dipoles) to a desired geometric transformation. The initial processing of motion/orientation cues of individual dots/dipoles of RDK/Glass patterns occur in early cortical areas such as V1/V2 – local processing (Dakin, 1997, Morrone, Burr & Vaina, 1995, Wilson & Wilkinson, 1998). This is followed by the global pooling of local motion/orientation resulting in the perception of overall direction/orientation of the whole pattern in the higher cortical such as MT for RDK (Morrone, Burr & Vaina, 1995) and V4 for Glass patterns (Dakin, 1997, Wilson & Wilkinson, 1998) – global processing. More recently, however, it has been suggested that interaction of information between motion and form is required for stable visual perception where motion information can help perceive form better or vice versa (Donato, Pavan & Campana, 2020, Goodale, 2011, Mather, et al., 2012, Ross, 2004, Ross, Badcock & Hayes, 2000, Sincich & Horton, 2005). The most dramatic example of how motion influences form perception is the demonstration of biological motion, where the biological form is only perceived when motion cues are introduced to the static pattern of dots (Johansson, 1973). Biological motion is believed to be processed along both motion and form processing channels but how much each channel is responsible for

* Corresponding author.
E-mail address: Mahesh.Joshi@plymouth.ac.uk (M.R. Joshi).

https://doi.org/10.1016/j.visres.2021.04.006
Received 5 October 2020; Received in revised form 23 April 2021; Accepted 23 April 2021
Available online 21 May 2021

the perception is still not clear (Giese & Poggio, 2003, Miller, Agnew & Pilz, 2018). Another stimulus that relies on such interaction between motion and form cues is the dynamic Glass pattern (Ross, Badcock & Hayes, 2000). Dynamic Glass patterns consist of sequential display of independent, random sets of static Glass patterns with the same general orientation (such as left translation) over time, this induces a compelling perception of motion (implied motion) along the axis of global orientation of static Glass patterns (Ross, Badcock & Hayes, 2000). The source of such perceived motion could only be from the underlying dipole orientation of static Glass pattern structures as coherent motion vectors are absent in dynamic Glass patterns.

The processing of implied motion is proposed to occur in areas V1 and V2 relying on a mechanism similar to motion streaks (Burr & Ross, 2002, Ross, 2004). Motion streaks are static image features that induce or accentuate the sense of motion, *e.g.* blurred static lines are frequently used by artists to provide the impression of motion direction in still images. Geisler (1999) proposed that moving objects leave a trail during temporal integration creating motion streaks. The visual system utilises these motion streaks (form information) to disambiguate object motion. The orientation selective cells in V1 are responsive to motion streaks. Additionally, the outputs of both orientation and motion selective cells in V1 are combined to form spatial motion direction (SMD) sensors that are sensitive to the orientation of the motion streak and the motion direction (Geisler, 1999). The dipoles in the dynamic Glass patterns ''approximate small line segments'' which form motion streaks and could stimulate the orientation selective and SMD detectors in V1 (Burr & Ross, 2002, Ross, 2004). The involvement of V1 and V2 neurones in decoding motion streaks in dynamic Glass patterns is further supported by the finding of a proportion of motion sensitive cells in monkeys and humans that are responsive to parallel motion (*i.e.* in the direction of their preferred orientation) instead of regularly encountered cells which are responsive to an orthogonal motion (Apthorp, et al., 2013, Geisler, et al., 2001). However, recent studies suggest that only local processing of dynamic Glass patterns *i.e.* orientation of dipole pairs occurs at V1 (Donato, Pavan & Campana, 2020, Krekelberg, Vatakis & Kourtzi, 2005, Ross, Badcock & Hayes, 2000) with global processing occurring through the motion and form interaction within higher extra striate areas such as MT (Kourtzi, Krekelberg & van Wezel, 2008, Li, et al., 2013, Mather et al., 2012, Pavan, Marotti & Mather, 2013). Imaging studies (Krekelberg, et al., 2003, Krekelberg, Vatakis & Kourtzi, 2005) reported that the motion selective cells in MT/MST respond similarly to the implied motion in dynamic Glass patterns and the real motion in RDK. The inability of MT/MST cells to differentiate between real and implied motion is why humans perceive motion in dynamic Glass patterns (Krekelberg et al., 2003, Krekelberg, Vatakis & Kourtzi, 2005).

Behavioural studies have compared coherence threshold for implied motion (dynamic Glass patterns) with thresholds for global form (static Glass patterns) and directional motion (RDK) to understand the processing mechanism and interactions between these visual functions (Day & Palomares, 2014, Nankoo, et al., 2012, Nankoo, et al., 2015). The coherence thresholds for dynamic Glass patterns are lower compared to static Glass patterns but higher than the real motion in RDK (Nankoo et al., 2012). The coherence thresholds for dynamic Glass patterns varied according to the pattern type (higher thresholds for translation compared to radial and rotational) similar to the static Glass patterns. This finding was reported as evidence of a larger influence of the form processing mechanism on implied motion processing (Nankoo et al., 2012). However, another study showed that the coherence thresholds reduced linearly with the increase in the temporal frequency of dynamic Glass patterns, suggesting that the processing mechanism relies more on the temporal properties (Day & Palomares, 2014). Hence the processing of implied motion and how it is influenced by motion and form processing mechanisms are still not clear. The coherence threshold is measured as the minimum fraction of signal elements required for the detection of coherent motion/orientation in the presence of random noise (Newsome & Pare, 1988). Another behavioural method that can be used to evaluate the processing of dynamic Glass patterns in relation to motion (RDK) and form (Glass patterns) processing is the equivalent noise paradigm (Watamaniuk & Sekuler, 1992). In the equivalent noise paradigm, the direction/orientation of individual elements is derived from a Gaussian distribution with a prescribed mean and standard deviation (Watamaniuk & Sekuler, 1992) where all individual elements are assigned with independent local directions/orientations along the mean of the underlying distribution. In such an arrangement, the dot/dipole elements act as signal (average direction/orientation of the elements) and noise (average dispersion of the individual element's direction/orientation from the mean) at the same time. Thresholds measured at variable noise can then be fit to a linear amplifier model of the equivalent noise paradigm to separate the observer's performance into internal noise and sampling efficiency parameters (Pelli, 1981, Pelli & Farell, 1999). For the RDK and Glass patterns, the internal noise derived from the equivalent noise paradigm represents the local variance in direction of motion (RDK) and orientation (Glass patterns) of individual elements – local processing (Dakin, Mareschal & Bex, 2005). The sampling efficiency meanwhile represents the number of elements the visual system summates to provide an overall global percept – global processing (Dakin, Mareschal & Bex, 2005). The equivalent noise paradigm can hence provide better insight into the interaction of motion and form processing at both local and global processing levels.

In this study, we adapted the equivalent noise paradigm to investigate sensitivity to implied motion and compared that to motion and form thresholds using physically equivalent stimuli in order to better understand the contribution of global motion and form on the perception of implied motion at local and global processing stages.

2. Methods

2.1. Participants

A total of 6 participants (mean age ± SD = 31.66 ± 6.86 years) with normal or corrected to normal visual acuity (6/6) participated in the study. Four of the six participants were naïve to the purpose of the experiment while two were psychophysically experienced observers. All participants provided written informed consent before participating in the experiments. The research was conducted in accordance with The Code of Ethics of the World Medical Association (Declaration of Helsinki) and approved by the Life Sciences Human Subjects Research Ethics Committee of Glasgow Caledonian University.

2.2. Stimuli

The global motion, global form, and implied motion were investigated using random dot kinematograms, Glass patterns, and dynamic Glass patterns respectively. The design of these stimuli has been described in detail in our previous studies (Joshi, Simmers & Jeon, 2016, Joshi, Simmers & Jeon, 2020). A brief description of method of stimulus generation and data collection is presented here. The stimuli were generated using MATLAB (MATLAB, 2009) with Psychophysics Toolbox extensions (Brainard, 1997, Kleiner, et al., 2007, Pelli, 1997) and displayed on a 21'' CRT monitor (resolution of 1920 × 1440 pixels and refresh rate of 75 Hz). The three stimuli shared the same physical characteristics. They were composed of 500 black dots (0.083° in diameter) presented in a circular aperture (10° in diameter at 50 cm) at the centre of the monitor with a dot density of 12.81 dots/deg^2. The mean background luminance of the display was 35 cd/m^2 and the contrast of the dot elements was 95% Michelson contrast.

2.3. RDKs

The RDKs were presented for 38 frames over the display time of 0.5 sec. All dots followed a defined trajectory for 6 frames (0.08 sec) at a dot speed of 10°/sec after which they disappeared and were generated at a

random location within the stimulus area.

2.4. Glass pattern

The Glass patterns were generated by randomly placing 250 black dots at the centre of the display. Another identical set of 250 dots was then superimposed after a linear geometrical transformation. The corresponding dot elements of the pattern were separated by a distance of 0.133°, which was scaled to the distance travelled by the dots in the RDK in two consecutive frames (dot speed of 10°/s for 0.5 sec with a monitor refresh rate of 75 frames/s).

2.5. Dynamic Glass pattern

Dynamic Glass patterns were composed of 9 independently generated static Glass patterns with similar physical parameters to that previously described for the static Glass patterns. Each static Glass pattern remained on the screen for 6 frames before being replaced by another independently generated static Glass pattern. The total stimulus duration was 0.5 s.

The direction of motion of individual dots in RDK and the orientation of component dipoles in Glass patterns, and dynamic Glass patterns were generated from a standard Gaussian distribution with a prescribed mean and standard deviation. The mean and standard deviation of the distribution were changed to vary the angle from the vertical reference (90°) and added external noise respectively across the trials. The global direction of motion of RDK and global orientation of Glass patterns (right or left from vertical) was randomised (Fig. 1). Eight external noise levels were used for the experiments: 0°, 2°, 4°, 8°, 16°, 24°, 32°, and 40°.

2.6. Procedure

The experiment started with the presentation of a white fixation dot (0.2° diameter) at the centre of the screen, followed by the presentation of either Glass patterns, dynamic Glass patterns or RDK for 0.5 sec. The participant's task in each trial was to discriminate the overall global orientation/implied motion/direction of the Glass pattern/dynamic Glass pattern/RDK from the vertical reference (90°). Only the negative response feedback was provided.

Eight 3:1 interleaved staircases (Wetherill and Levitt, 1965) were used for stimulus presentation and data collection. The staircase for each external noise level started with an overall mean orientation or direction of 30° from the vertical. The initial step size for stimulus intensity adjustment was an octave which was reduced to half an octave and further to a quarter of an octave after three and six reversals respectively. Each staircase terminated after the completion of ten reversals or 100 trials, whichever occurred first and the threshold was calculated as the geometrical mean of the last seven reversals. Each Participant completed five sessions of psychophysical experiment for three stimuli binocularly after completing two practice sessions that consisted of 15 trials for each noise level.

The thresholds (τ_o) at eight external noise levels (σ_{ext}) were modelled by the equation below to relate the performance into internal equivalent noise (σ_{eq}) and sampling efficiency (*Eff*) parameters (Pelli, 1981, Pelli & Farell, 1999).

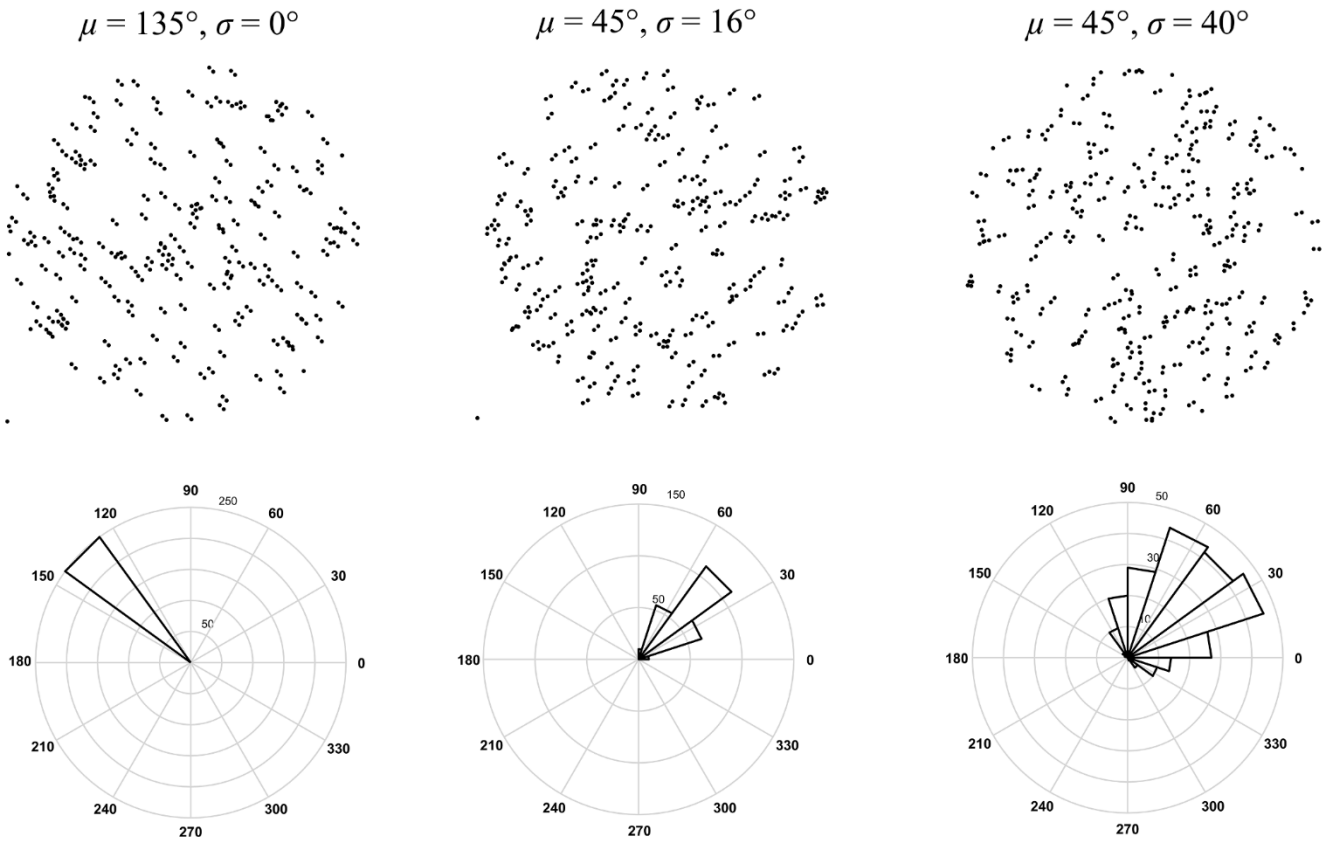

Fig. 1. Examples of Glass patterns with differing orientation and noise levels (top panels). The orientations of individual dipoles in each Glass pattern were generated from a Gaussian distribution (shown in angle histograms, bottom panels). The mean (μ) of the distribution (±45° from the vertical here) represents the global orientation of the Glass patterns. The added external noise was varied by changing the standard deviation (σ) of the distribution (from left to right panels, 0°, 16°, and 40°). The task for the observer was to discriminate the overall orientation of Glass patterns. For the RDK, individual dots followed the directional trajectory generated from the Gaussian distribution. For dynamic Glass patterns, nine frames of independent static Glass patterns were displayed over the stimulus duration.

$$\tau_o = \sqrt{\frac{\sigma_{eq}^2 + \sigma_{ext}^2}{Eff}} \quad (1)$$

The threshold data were then used to fit various nested models. The full model contained six parameters (2 each of σ_{eq} and *Eff* for Glass patterns, dynamic Glass patterns, and RDK). The fitting models were then reduced by constraining the parameters (either σ_{eq} and *Eff* or both across the three stimuli), resulting in different nested models. The best model to describe the threshold data was selected by testing the goodness of fits between the nested models hierarchically with the following equation.

$$F(df_1, df_2) = \frac{r_{full}^2 - r_{reduced}^2/df_1}{1 - r_{full}^2/df_2} \quad (2)$$

Where, $df_1 = k_{\text{full}} - k_{\text{reduced}}$ and $df_2 = N - k_{\text{full}}$. k is the number of parameters in each model, and N is the number of predicted data points.

3. Results

The mean implied motion thresholds for dynamic Glass patterns (*d*Glass) were higher than the mean thresholds for the RDK but lower than those for the Glass patterns at all external noise levels (Fig. 2). For all stimuli, when thresholds were plotted against the external noise in the logarithmic scale, thresholds were low and similar at lower noise levels and started to increase at noise levels of 8° and 16° with the highest thresholds for the 40° variance.

The individual and mean thresholds were used to fit the linear amplifier model. Various nested models were tested from the full model (with 3 sets of independent σ_{eq} and *Eff*) to the most parsimonious model (with a single set of σ_{eq} and *Eff*) across the three stimuli (see Table 1 and Fig. 3).

Among the reduced models for mean thresholds, the goodness of fit (r^2) with one σ_{eq} and three *Eff* was equivalent to the full model (three σ_{eq} and three *Eff*) ($F(2,18) = 1.10$, $p > 0.1$). The fits with three σ_{eq} and one *Eff* ($F(2,18) = 42.92$, $p < 0.01$) and one σ_{eq} and one *Eff* ($F(2,18) = 49.07$, $p < 0.01$) meanwhile resulted in poorer fits compared to the full model. A further test with one σ_{eq} and three *Eff* as the full model and one σ_{eq} and one *Eff* as the reduced model showed that the reduced model resulted in a significantly poorer fit ($F(2,20) = 107.83$, $p < 0.01$). The same pattern of result was obtained for all individual observers. (Table 1) The result confirmed that the model with one σ_{eq} and three *Eff* best described the performance of the observers across the three stimulus types.

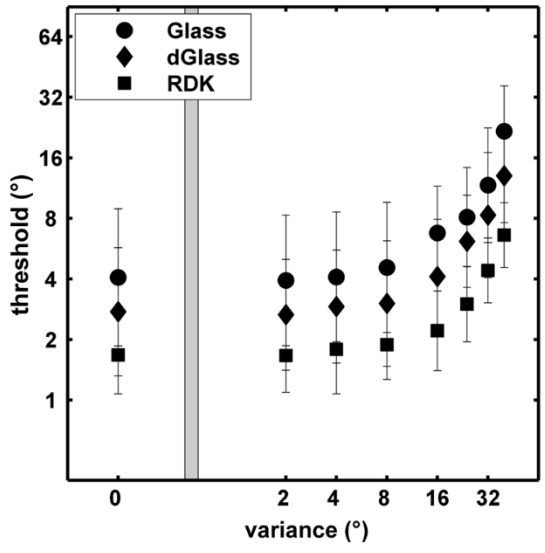

Fig. 2. Mean orientation/implied motion/directional motion discrimination thresholds ($n = 6$) at eight noise levels for Glass patterns, dynamic Glass patterns and RDK. The error bar represents ± 1standard deviation and the grey bar represents axis break.

4. Discussion

4.1. Global motion vs. Global form

The mean fine discrimination thresholds (*i.e.*, discrimination threshold from the vertical at no noise condition) for the direction of motion in the RDK and the orientation of the dipole Glass patterns were 1.85° (±0.89°) and 5.62° (±5.76°) respectively. These results are similar to fine motion direction discrimination thresholds reported for young adults in previous studies (Bocheva, Angelova & Stefanova, 2013, Bogfjellmo, Bex & Falkenberg, 2014). As far as we are aware there are no reports on fine orientation discrimination thresholds using Glass patterns. The orientation discrimination thresholds (Glass patterns) were consistently higher than that for the direction of motion (RDK) at all levels of added external noise which is in line with previous studies measuring coherence threshold using physically comparable Glass patterns (Ditchfield, McKendrick & Badcock, 2006, Nankoo et al., 2012) and line streaks (Simmers, Ledgeway & Hess, 2005, Simmers, et al., 2003, Simmers, et al., 2006). We further probed the better performance for motion processing with the equivalent noise paradigm to parse out the effects of local and global processing mechanisms. Internal equivalent noise and sampling efficiency for the mean direction discrimination thresholds were 12.86° and 8 elements respectively. Previous studies have reported the internal noise in the motion domain ranging from 2.97° to 25° (Bocheva, Angelova & Stefanova, 2013, Dakin, Mareschal & Bex, 2005, Watamaniuk & Sekuler, 1992). The difference might be reflective of the stimulus differences in these studies as has been reported before (Bocheva, Angelova & Stefanova, 2013, Dakin, Mareschal & Bex, 2005). There are no previous reports on the internal noise and sampling efficiency employing Glass patterns. A study using Gabor patches reported equivalent internal noise in the range of 4.4°–7.8° (Dakin, 2001).

Our result of similar internal equivalent noise in motion and form domains suggests that both pathways might share similar local processing limitations with differences in the performance due to the improved efficiency in the global motion processing mechanism. Various studies suggest that the local processing of dot motion in RDK (Morrone, Burr & Vaina, 1995; Nishida, 2011) and dipole orientation in Glass patterns (Smith, Bair & Movshon, 2002, Smith, Kohn & Movshon, 2007, Wilson & Wilkinson, 1998, Wilson, Wilkinson & Asaad, 1997, Wilson, Switkes & De Valois, 2004) occur in area V1/V2 with global processing occurring in areas of MT and V4. The common physiological limitations in the local processing area could have resulted in the similar internal equivalent noise observed in both domains. The sampling efficiency parameter refers to the visual system's ability to pool local directional/orientation information from the individual dot and dipole elements (Dakin, Mareschal & Bex, 2005). Another method used to study the pooling of motion/orientation signals is by restricting the coherent elements in the RDK and Glass patterns to wedge shaped areas of varying size within the stimulus. The discrimination threshold for a translation RDK improved linearly with the increase in the size of the signal area, implying global spatial summation of almost 100% (Morrone, Burr & Vaina, 1995) while for the translation Glass patterns, the global summation ranged between 25 and 33% (Wilson & Wilkinson, 1998). The better sampling efficiency along the motion pathway in the current study albeit using a different experimental paradigm is in line with the previous findings of a larger global pooling for motion processing than form processing (Morrone, Burr & Vaina, 1995, Wilson & Wilkinson, 1998).

4.2. Implied motion vs. Global motion vs. Global form

The implied motion thresholds for the dynamic Glass patterns were

Table 1
The best fitting parameters and r^2 values for model fits to individual and mean threshold data for Glass, *d*Glass, and RDK.

Participants	S1	S2	S3	S4	S5	S6	Average
Full model							
σ_{eq} Glass	11.05°	24.91°	9.24°	5.22°	9.51°	8.95°	10.06°
σ_{eq} *d*Glass	10.45°	12.24°	10.01°	8.44°	12.38°	9.01°	10.32°
σ_{eq} RDK	10.39°	16.61°	13.22°	8.65°	19.45°	12.50°	12.86°
Eff Glass	1.51	2.56	2.40	3.75	3.46	3.38	2.64
*Eff d*Glass	3.19	3.30	1.80	7.83	4.90	5.48	3.97
Eff RDK	5.77	8.64	6.87	7.92	8.63	11.40	7.91
r^2	0.94	0.94	0.95	0.94	0.83	0.97	0.97
Reduced model-1 with σ_{eq} constrained							
σ_{eq}	10.63°	16.91°	10.75°	7.27°	12.70°	10.06°	11.00°
Eff Glass	1.48	1.97	2.58	4.29	4.03	3.58	2.76
*Eff d*Glass	3.22	3.99	1.86	7.32	4.97	5.78	4.10
Eff RDK	5.83	8.74	6.15	7.31	6.67	10.10	7.27
r^2	0.94	0.90	0.94	0.92	0.80	0.96	0.96
F(2,18)	0.03*	2.12*	1.06*	2.30*	1.92*	2.19*	1.10*
Reduced model-2 with *Eff* constrained							
σ_{eq} Glass	38.95°	67.54°	17.98°	10.51°	15.68°	24.73°	23.10°
σ_{eq} *d*Glass	13.33°	26.51°	26.22°	6.42°	13.38°	12.30°	13.55°
σ_{eq} RDK	6.32°	10.83°	6.92°	6.60°	10.69°	7.06°	7.33°
Eff	3.89	5.99	3.94	6.29	5.21	6.99	4.92
r^2	0.81	0.83	0.75	0.84	0.71	0.80	0.81
F(2,18)	19.32	11.13	33.32	14.89	6.85	48.84	42.92
Simplest model with both σ_{eq} and *Eff* constrained							
σ_{eq}	10.63°	16.91°	10.75°	7.27°	12.70°	10.06°	11.00°
Eff	3.03	4.10	3.09	6.12	5.11	5.94	4.35
r^2	0.45	0.25	0.49	0.81	0.67	0.59	0.61
F(2,18)†	37.34	39.20	38.74	9.73	4.31	55.22	49.07
F(2,20)‡	82.96	84.75	84.91	19.06	7.44	120.28	107.83

The values in the top section are the results of the fits with six free parameters (one σ_{eq} and *Eff* each for Glass, *d*Glass, and RDK). The second and third sections show the results with σ_{eq} and *Eff* fixed respectively across Glass, *d*Glass, and RDK. The bottom section shows results with both σ_{eq} and *Eff* fixed across the conditions. The *F* scores are the result of a nested hypothesis test between restricted models (4-parameter or 2-parameter models) and the full models (6-parameter or 4-parameter models).
* = *F* scores which resulted in no significant difference ($p > 0.05$) in the goodness of the fit measure with the reduced model (here 1 σ_{eq}, 3 *Eff*) compared to the full model (3 σ_{eq}, 3 *Eff*). The rest of the *F* scores represent a poorer fit ($p < 0.05$) compared to the full model (3 σ_{eq}, 3 *Eff*).
† = *F* statistics of the simplest model (1 σ_{eq}, 1 *Eff*) compared to full model (3 σ_{eq}, 3 *Eff*).
‡ = *F* statistics of the simplest model (1 σ_{eq}, 1 *Eff*) compared to the model selected from the first stage of comparison (1 σ_{eq}, 3 *Eff*).

lower than those for the static Glass patterns but higher than the RDK at all external noise levels. As far as we know, no study has evaluated the sensitivity to dynamic Glass patterns using the equivalent noise paradigm. Other studies have reported lower coherence thresholds for dynamic Glass patterns compared to the static Glass patterns (Burr & Ross, 2006, Nankoo et al., 2012, Nankoo et al., 2015). The reduced thresholds for the dynamic Glass patterns could be due to the activation of the motion streak mechanism (Ross, 2004, Ross, Badcock & Hayes, 2000) that may be present at the early cortical visual areas of V1 and V2 (Apthorp et al., 2013, Burr & Ross, 2002) and the later global processing areas of MT and MST (Krekelberg, Vatakis & Kourtzi, 2005, Mather et al., 2012, Pavan, Marotti & Mather, 2013). Another possible reason for better sensitivity to implied motion in dynamic Glass patterns compared to the static Glass patterns could be due to the summation of information from multiple independent static Glass patterns over time (Nankoo et al., 2015). Two factors are involved in such improvement: the accumulation of form information from multiple static Glass patterns (Nankoo et al., 2012, Nankoo et al., 2015) and the influence of temporal frequency of the presentation (Day & Palomares, 2014). The coherence thresholds for the dynamic Glass patterns varied according to the pattern types (translation, radial, and rotation) as observed for the static Glass patterns while the motion coherence thresholds were similar for all three RDK types (Nankoo et al., 2012). The result hence emphasised a larger role for the form processing mechanism (Nankoo et al., 2012). However, other studies have reported that the motion coherence thresholds for RDK also vary depending upon the pattern types, especially at slower speeds (Freeman & Harris, 1992, Lee & Lu, 2010). In another study, coherence thresholds for dynamic Glass patterns reduced linearly with the increase in temporal frequency suggesting the importance of temporal properties (Day & Palomares, 2014). However, on independently varying the temporal frequency and the number of unique frames, the number of frames was still more influential in threshold reduction (Nankoo et al., 2015).

The similar level of internal noise observed for different stimuli (RDK, dynamic Glass and Glass patterns) suggests that local processing (in both motion and form domains) may share a common local level processing of dot motion and dipole orientation. The finding that the perception of both static and dynamic Glass patterns are lost when the dipoles are of opposite polarity (Or, Khuu & Hayes, 2007) further suggests that both patterns share similar local level processing. Motion streak detectors present in the primary visual cortex are proposed to be responsible for the processing of implied motion in line streaks (Geisler, 1999). The similar internal noise observed here between dynamic Glass patterns and static Glass patterns in which motion streak is absent and between dynamic Glass and RDK in which motion streak detectors would be more influential suggests that motion streak mechanism in V1 might not be adequate to explain the implied motion perceived in dynamic Glass patterns.

The difference in the performance for three stimulus types was best represented by the change in the global processing parameter, the sampling efficiency. The motion sensitive cells in MT/MST respond similarly to both real motion and implied motion (Krekelberg et al., 2003, Krekelberg, Vatakis & Kourtzi, 2005) and may well be involved in the global processing of the implied motion in dynamic Glass patterns. The motion-form interactions similar to that proposed for the motion streak mechanism are also present at the global processing levels of MT (Mather et al., 2012) and MST (Pavan, Marotti & Mather, 2013), and such interactions could have influenced the differences in the sampling efficiency observed here. Furthermore, some MT cells responsive to orthogonal motion, change their preference over time to that of parallel

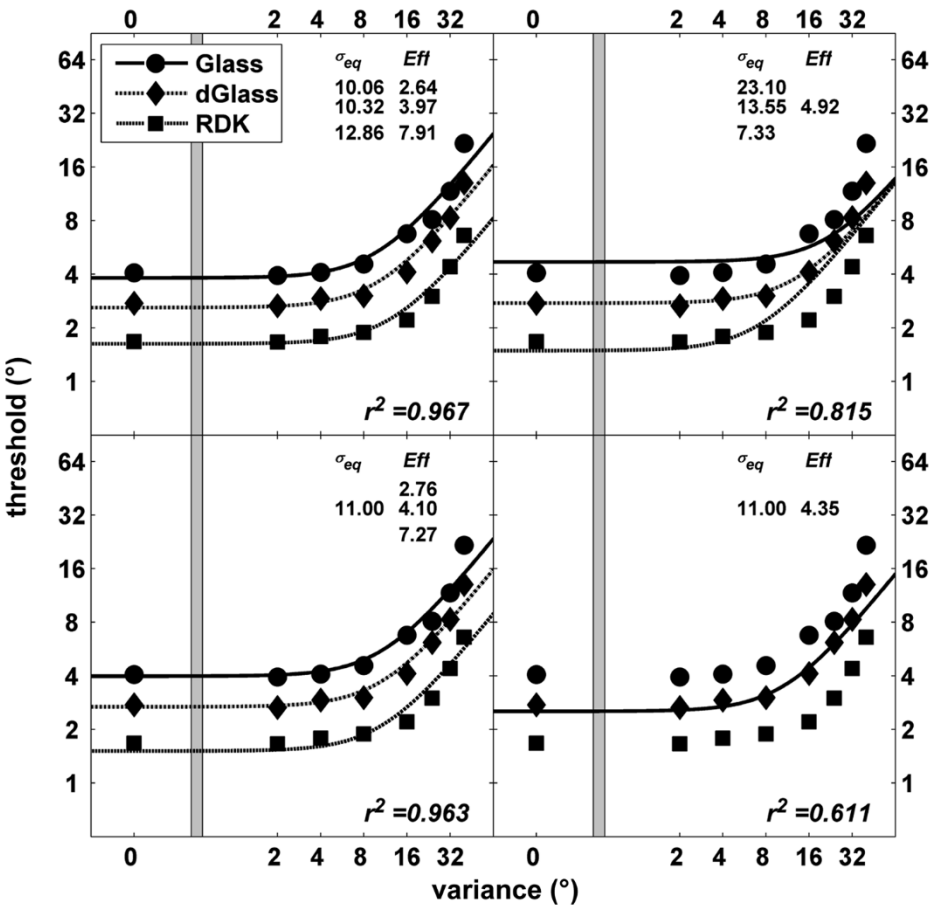

Fig. 3. Nested models relating the mean thresholds to internal noise and sampling efficiency for Glass, *d*Glass, and RDK. Top left: the full model with independent σ_{eq} and *Eff* for three stimuli. Top right: the constrained model with independent σ_{eq} and a single *Eff* parameter. Bottom left: the constrained model with independent *Eff* and a single σ_{eq} parameter. Bottom right: the simplest reduced model with both σ_{eq} and *Eff* constrained. The reduced model with one σ_{eq} and three *Eff* (bottom left) resulted in no significant difference ($p > 0.05$) in the goodness of the fit measure (r^2) compared to the full model.

motion (in the direction of the motion streak) starting from around 75 ms of the stimulus onset (Pack & Born, 2001). This change in sensitivity could be influential in processing the motion streaks left behind by the fast moving objects (Burr & Ross, 2002). Our results show that any facilitation of implied motion processing due to the interaction of motion and form processing streams in line with the motion streak mechanism may well extend to the global processing level. However, the mechanism may not be as efficient as that for directional motion in RDK. From our results of constant internal noise and a difference in sampling efficiency and previous literature, we speculate that the local processing of dipole orientation in dynamic Glass patterns is similar to the processing of static Glass patterns (extracting dipole orientation) with further global processing most likely occurring along the motion processing areas of MT/MST. Such an assumption is supported by a series of imaging and motion adaptation studies. Imaging studies report that the motion responsive neurones along the ventral stream are not responsive to the implied motion in dynamic Glass patterns (Krekelberg et al., 2003, Krekelberg, Vatakis & Kourtzi, 2005) suggesting that any contribution from the form processing pathway to the processing of dynamic Glass patterns is mostly limited to the local extraction of dipole orientation. The notion of the involvement of MT in global processing of dynamic Glass patterns is also supported by adaptation studies. The perceived direction of motion streaks is affected by adaptation to a wide range of static orientations (Tang, et al., 2015). This range was broader than what could be accounted for by the neuronal properties of V1. Furthermore, this range closely approximated the broad bandwidths of motion selective cells in area MT. Based on these findings an alternate model was proposed, where the orientation cues are initially processed at the V1 level with the second stage of motion processing occurring at area MT (Tang et al., 2015). The model predictions are in line with our findings of similar internal equivalent noise and differences in sampling efficiency for dynamic Glass patterns compared to both RDK and static Glass patterns.

Our results show that humans have better sensitivity to global implied motion compared to global form but lower than that for global motion. The results further suggest that higher thresholds for implied motion compared to real motion is due to differences in sampling efficiency which could be due to inefficient pooling of local cues of implied motion at the global processing stage.

CRediT authorship contribution statement

Mahesh R. Joshi: Conceptualization, Methodology, Software, Formal analysis, Investigation, Writing - original draft. **Anita J. Simmers:** Methodology, Resources, Writing - review & editing, Supervision. **Seong T. Jeon:** Methodology, Software, Resources, Writing - review & editing, Supervision.

References

Apthorp, D., Schwarzkopf, D. S., Kaul, C., Bahrami, B., Alais, D., & Rees, G. (2013). Direct evidence for encoding of motion streaks in human visual cortex. *Proceedings of the Royal Society B: Biological Sciences, 280*(1752), 20122339.

Bocheva, N., Angelova, D., & Stefanova, M. (2013). Age-related changes in fine motion direction discriminations. *Experimental Brain Research, 228*(3), 257–278.

Bogfjellmo, L.G., Bex, P.J., & Falkenberg, H.K. (2014). The development of global motion discrimination in school aged children. Journal of Vision, 14 (2).

Braddick, O., Atkinson, J., & Wattam-Bell, J. (2003). Normal and anomalous development of visual motion processing: Motion coherence and 'dorsal-stream vulnerability'. *Neuropsychologia, 41*(13), 1769–1784.

Braddick, O. J., O'Brien, J. M. D., Wattam-Bell, J., Atkinson, J., Hartley, T., & Turner, R. (2001). Brain areas sensitive to coherent visual motion. *Perception, 30*(1), 61–72.

Braddick, O.J., O'Brien, J.M.D., Rees, G., Wattam-Bell, J., Atkinson, J., & Turner, R. (2002). Quantitative neural responses to form coherence in human extrastriate cortex. Society for Neuroscience 32nd Annual Meeting (Washington, DC.

Brainard, D. H. (1997). The Psychophysics Toolbox. *Spatial Vision, 10*(4), 433–436.

Burr, D., & Ross, J. (2006). The effects of opposite-polarity dipoles on the detection of Glass patterns. *Vision Res, 46*(6-7), 1139–1144.
Burr, D. C., & Ross, J. (2002). Direct Evidence That "Speedlines" Influence Motion Mechanisms. *The Journal of Neuroscience, 22*(19), 8661–8664.
Dakin, S. C. (1997). The detection of structure in glass patterns: Psychophysics and computational models. *Vision Research, 37*(16), 2227–2246.
Dakin, S. C. (2001). Information limit on the spatial integration of local orientation signals. *Journal of the Optical Society of America. A, Optics, image science, and vision, 18*(5), 1016–1026.
Dakin, S. C., Mareschal, I., & Bex, P. J. (2005). Local and global limitations on direction integration assessed using equivalent noise analysis. *Vision Research, 45*(24), 3027–3049.
Day, A. M., & Palomares, M. (2014). How temporal frequency affects global form coherence in Glass patterns. *Vision Research, 95*, 18–22.
Ditchfield, J. A., McKendrick, A. M., & Badcock, D. R. (2006). Processing of global form and motion in migraineurs. *Vision Research, 46*(1-2), 141–148.
Donato, R., Pavan, A., & Campana, G. (2020). Investigating the interaction between form and motion processing: A review of basic research and clinical evidence. *Frontiers in Psychology, 11*(2867).
Freeman, T. C. A., & Harris, M. G. (1992). Human sensitivity to expanding and rotating motion: Effects of complementary masking and directional structure. *Vision Research, 32*(1), 81–87.
Geisler, W. S. (1999). Motion streaks provide a spatial code for motion direction. *Nature, 400*(6739), 65–69.
Geisler, W. S., Albrecht, D. G., Crane, A. M., & Stern, L. (2001). Motion direction signals in the primary visual cortex of cat and monkey. *Visual Neuroscience, 18*(4), 501–516.
Giese, M. A., & Poggio, T. (2003). Neural mechanisms for the recognition of biological movements. *Nature Reviews Neuroscience, 4*(3), 179–192.
Glass, L. (1969). Moire effect from random dots. *Nature, 223*(5206), 578–580.
Goodale, M. A. (2011). Transforming vision into action. *Vision Research, 51*(13), 1567–1587.
Johansson, G. (1973). Visual perception of biological motion and a model for its analysis. *Perception & Psychophysics, 14*(2), 201–211.
Joshi, M. R., Simmers, A. J., & Jeon, S. T. (2016). Concurrent investigation of global motion and form processing in amblyopia: An equivalent noise approachglobal motion and form processing in amblyopia. *Investigative Ophthalmology & Visual Science, 57*(11), 5015–5022.
Joshi, M.R., Simmers, A.J., & Jeon, S.T. (2020). Implied Motion From Form Shows Motion Aids the Perception of Global Form in Amblyopia. Investigative Ophthalmology & Visual Science, 61 (5), 58-58.
Kleiner, M., Brainard, D., Pelli, D., Ingling, A., Murray, R., & Broussard, C. (2007). What's new in Psychtoolbox-3? *Perception, 36*, 1–16.
Kourtzi, Z., Krekelberg, B., & van Wezel, R. J. A. (2008). Linking form and motion in the primate brain. *Trends in Cognitive Sciences, 12*(6), 230–236.
Krekelberg, B., Dannenberg, S., Hoffmann, K.-P., Bremmer, F., & Ross, J. (2003). Neural correlates of implied motion. *Nature, 424*(6949), 674–677.
Krekelberg, B., Vatakis, A., & Kourtzi, Z. (2005). Implied motion from form in the human visual cortex. *Journal of Neurophysiology, 94*(6), 4373–4386.
Lee, A.L., & Lu, H. (2010). A comparison of global motion perception using a multiple-aperture stimulus. Journal of Vision, 10 (4), 9 1-16.
Li, P., Zhu, S., Chen, M., Han, C., Xu, H., Hu, J., … Lu, H. (2013). A motion direction preference map in monkey V4. *Neuron, 78*(2), 376–388.
Livingstone, M. S., & Hubel, D. H. (1987). Psychophysical evidence for separate channels for the perception of form, color, movement, and depth. *The Journal of Neuroscience, 7*(11), 3416–3468.
Mather, G., Pavan, A., Bellacosa, R. M., & Casco, C. (2012). Psychophysical evidence for interactions between visual motion and form processing at the level of motion integrating receptive fields. *Neuropsychologia, 50*(1), 153–159.
MATLAB. (2009). *version 7.9.0.529* ((R2009b).). (Natick, Massachusetts: The MathWorks Inc.
Miller, L., Agnew, H. C., & Pilz, K. S. (2018). Behavioural evidence for distinct mechanisms related to global and biological motion perception. *Vision Research, 142*, 58–64.
Milner, A. D., & Goodale, M. A. (2008). Two visual systems re-viewed. *Neuropsychologia, 46*(3), 774–785.
Morrone, M. C., Burr, D. C., & Vaina, L. M. (1995). Two stages of visual processing for radial and circular motion. *Nature, 376*(6540), 507–509.
Nankoo, J.-F., Madan, C. R., Spetch, M. L., & Wylie, D. R. (2012). Perception of dynamic Glass patterns. *Vision Research, 72*, 55–62.
Nankoo, J.-F., Madan, C. R., Spetch, M. L., & Wylie, D. R. (2015). Temporal summation of global form signals in dynamic Glass patterns. *Vision Research, 107*, 30–35.
Newsome, W. T., & Pare, E. B. (1988). A selective impairment of motion perception following lesions of the middle temporal visual area (MT). *The Journal of Neuroscience, 8*(6), 2201–2211.
Nishida, S.y. (2011). Advancement of motion psychophysics: Review 2001–2010. Journal of Vision, 11 (5), 11-11.
Or, C. C.-F., Khuu, S. K., & Hayes, A. (2007). The role of luminance contrast in the detection of global structure in static and dynamic, same- and opposite-polarity Glass patterns. *Vision Research, 47*(2), 253–259.
Pack, C. C., & Born, R. T. (2001). Temporal dynamics of a neural solution to the aperture problem in visual area MT of macaque brain. *Nature, 409*(6823), 1040–1042.
Pavan, A., Marotti, R.B., & Mather, G. (2013). Motion-form interactions beyond the motion integration level: Evidence for interactions between orientation and optic flow signals. Journal of Vision, 13 (6), 16-16.
Pelli, D.G. (1981). Effects of Visual Noise. PhD (Cambridge: Cambridge University.
Pelli, D. G. (1997). The VideoToolbox software for visual psychophysics: Transforming numbers into movies. *Spatial Vision, 10*(4), 437–442.
Pelli, D. G., & Farell, B. (1999). Why use noise? *Journal of the Optical Society of America A, Optics, image science, and vision, 16*(3), 647–653.
Ross, J. (2004). The perceived direction and speed of global motion in Glass pattern sequences. *Vision Research, 44*(5), 441–448.
Ross, J., Badcock, D. R., & Hayes, A. (2000). Coherent global motion in the absence of coherent velocity signals. *Current Biology, 10*(11), 679–682.
Simmers, A. J., Ledgeway, T., & Hess, R. F. (2005). The influences of visibility and anomalous integration processes on the perception of global spatial form versus motion in human amblyopia. *Vision Research, 45*(4), 449–460.
Simmers, A. J, Ledgeway, T., Hess, R. F, & McGraw, P. V (2003). Deficits to global motion processing in human amblyopia. *Vision Research, 43*(6), 729–738.
Simmers, A. J., Ledgeway, T., Mansouri, B., Hutchinson, C. V., & Hess, R. F. (2006). The extent of the dorsal extra-striate deficit in amblyopia. *Vision Research, 46*(16), 2571–2580.
Sincich, L. C., & Horton, J. C. (2005). The circuitry of V1 and V2: Integration of color, form, and motion. *Annual Review of Neuroscience, 28*(1), 303–326.
Smith, M. A., Bair, W., & Movshon, J. A. (2002). Signals in macaque striate cortical neurons that support the perception of glass patterns. *The Journal of Neuroscience, 22*(18), 8334–8345.
Smith, M. A., Kohn, A., & Movshon, J. A. (2007). Glass pattern responses in macaque V2 neurons. *Journal of Vision, 7*(3), 5. https://doi.org/10.1167/7.3.510.1167/7.3.5.M110.1167/7.3.5.M2.
Tang, M. F., Dickinson, J. E., Visser, T. A. W., & Badcock, D. R. (2015). The broad orientation dependence of the motion streak aftereffect reveals interactions between form and motion neurons. *Journal of Vision, 15*(13), 4. https://doi.org/10.1167/15.13.410.1167/15.13.4.M110.1167/15.13.4.M2.
Watamaniuk, S. N. J., & Sekuler, R. (1992). Temporal and spatial integration in dynamic random-dot stimuli. *Vision Research, 32*(12), 2341–2347.
Wilson, H. R, & Wilkinson, F. (1998). Detection of global structure in Glass patterns: Implications for form vision. *Vision Research, 38*(19), 2933–2947.
Wilson, H. R., Wilkinson, F., & Asaad, W. (1997). Concentric orientation summation in human form vision. *Vision Research, 37*(17), 2325–2330.
Wilson, J. A, Switkes, E, & De Valois, R. L (2004). Glass pattern studies of local and global processing of contrast variations. *Vision Research, 44*(22), 2629–2641.